# Heating through the glass transition: A rigidity approach to the boson peak

Hugo M. Flores-Ruiz and Gerardo G. Naumis
*Instituto de Física, Universidad Nacional Autónoma de México (UNAM), Apartado Postal 20-364, 01000 México Distrito Federal, Mexico*

J. C. Phillips
*Department of Physics and Astronomy, Rutgers University, Piscataway, New Jersey 08854-8019, USA*
(Received 22 October 2010; published 2 December 2010)

Using molecular dynamics, we study the relationship between the excess of low-frequency vibrational modes (Boson peak, BP) and the glass transition for a bidispersive glass interacting through a truncated Lennard-Jones potential. The evolution of the BP with increasing temperature is correlated with the average coordination, as predicted by rigidity theory. This is due to a lack of atomic "contacts," as is confirmed by taking a crystal with broken bonds. We show how the quadratic mean displacement ($\langle u^2 \rangle$) is enhanced by the BP. When $\langle u^2 \rangle$ is obtained on short time scales or measured on inherent structures, the glass transition temperature $T_g$ is determined by the position and height of the BP. Between the melting temperature $T_m$ and $T_g$, the nature of the relaxation processes exhibit phase separation, where the backbone increases its rigidity while the smaller atoms diffuse away to form separate crystals.

DOI: 10.1103/PhysRevB.82.214201 PACS number(s): 64.70.kj, 64.70.Q−, 61.43.Fs

## I. INTRODUCTION

The process of glass formation (or avoidance of phase separation and crystallization) is still controversial,[1,2] for example, the nature of the relaxation processes between $T_m$ and $T_g$.[3–5] Even when a glass is already formed, some questions remain open in the sense that there is no consensus on what is the "right answer." For example, almost all glasses present a large "soft" excess of low-frequency vibrational modes (LFVM) when compared with crystals.[6] One type of excess is a broad maximum called the Boson peak (BP), which appears at frequencies ($\omega$) on the order of a terahertz. The other is the presence of floppy modes in network glasses. While there is no consensus about the nature of the BP,[7] the appearance of floppy modes can be very successfully explained by the Phillips-Thorpe rigidity theory (RT).[8,9] Usually both anomalies are considered as different phenomena, but as we will show here, there is a certain commonality between both phenomena.

In RT, atomic bonds are considered as mechanical constraints,[8] i.e., as structural hinges and rods. Floppy modes are due to the low coordination of the system because the number of constraints ($N_c$) is less than the number of configurational degrees of freedom[8,9] ($3N$, where $N$ is the number of atoms). As a result, there are not enough constraints to avoid particle displacements and make the system rigid.[8,9] Rigid systems where $N_c=3N-6$ are known as isostatic. Some glasses can even self-organize in isostatic networks to reduce stress.[10–12] Indeed, the lack of constraints has been recognized as a relevant aspect in many other fields, such as colloids, granular matter, foams, jamming transition,[13–19] and there are some hints that the BP has it origins in such lack of constraints.[13]

LFVM anomalies are present in the specific heats almost all glasses,[6] but only recently this observation has been taken into account in the understanding of glass formation. In a series of previous papers,[20–22] we have shown that floppy modes can determine $T_g$ and relaxation properties. Here we employ RT to establish the relationship between BP and $T_g$. Within RT, the average connectivity of the network,[8] usually described by the average coordination number ($\langle Z \rangle$), plays a key role. Here we show how the BP is correlated with $\langle Z \rangle$ in a binary Lennard-Jones glass. Then $T_g$ can be obtained from the excess of LFVM by looking at the mean quadratic displacement ($\langle u^2(T) \rangle$) and the Lindemann criteria[20] for $T_m$ and $T_g \sim 2T_m/3$. The evolution of $\langle Z \rangle$ also sheds light on the nature of the relaxation processes between $T_g$ and $T_m$. There are two keys aspects to obtain the present results: the use of a *finite-range potential* in order to be able to define unambiguously what is a bond (constraint) between atoms,[23] and *progressive heating of the glass*, instead of supercooling, as almost all other works do.

## II. GLASS MODEL AND MOLECULAR DYNAMICS DETAILS

As our glass model we used the standard binary mixture of particles $A$ and $B$, all having the same mass $m$. The interactions between particles are given by a purely repulsive potential,[23]

$$\Phi_{\alpha\beta}(r_{ij}) = \begin{cases} 4\epsilon_{\alpha\beta}\left[\left(\frac{\sigma_{\alpha\beta}}{r_{ij}}\right)^{12} - \left(\frac{\sigma_{\alpha\beta}}{r_{ij}}\right)^{6}\right] + \epsilon_{\alpha\beta} & \text{if } r_{ij} \le r_{\alpha\beta}^{c} \\ 0 \text{ in any other case} \end{cases}, \tag{1}$$

where $r_{ij}$ is the interparticle distance, $\epsilon_{\alpha\beta}$ is a constant energy, and $r_{\alpha\beta}^{c}=2^{1/6}\sigma_{\alpha\beta}$ is the cut-off radius. The parameters $\epsilon_{\alpha\beta}$ and $\alpha_{\alpha\beta}$ were chosen as follows:[23] $\sigma_{AA}=1.0$, $\epsilon_{AA}=1.0$, $\sigma_{AB}=0.88$, $\epsilon_{AB}=1.5$, $\sigma_{BB}=0.8$, and $\epsilon_{BB}=0.5$, which inhibits crystallization. The simulations were made using molecular dynamics at constant volume and temperature. The units of mass, length, time, pressure, and temperature are $m$, $\sigma_{AA}$, $\tau=\sigma_{AA}\sqrt{m/\epsilon_{AA}}$, $\epsilon_{AA}/\sigma_{AA}^3$, and $\epsilon_{AA}/k_B$, respectively, with $k_B$ being Boltzmann's constant. The simulations were performed

 

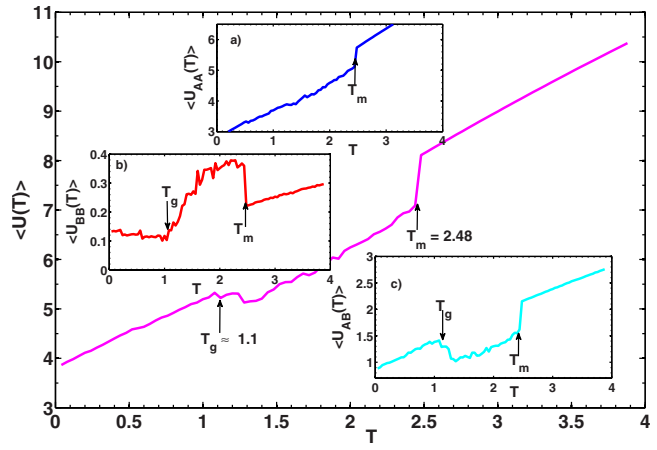


FIG. 1. (Color online) Total internal energy $\langle U\rangle=\langle U_{AA}\rangle+\langle U_{BB}\rangle+\langle U_{AB}\rangle$ versus temperature $T$. Insets: (a) energy of $A$-$A$ bonds, (b) $B$-$B$ bonds, and (c) $A$ and $B$ bonds.

with $N=864$ particles. We used a 80:20 mixture of $A$ and $B$ particles. The glass was produced by supercooling following standard procedures:[23] we heated a doped crystal up to fluid state, and then we cooled it at velocity $\gamma=dT/dt=0.2$ until it was in a solid amorphous state. Once the glass was obtained, the initial configuration was heated at three different heating rates $\gamma_0=0.005$, $\gamma_1=0.02$, and $\gamma_2=0.1$.

## III. RESULTS

Figure 1 shows $\langle U\rangle$ as a function of $T$ using $\gamma_1$ as the heating rate (similar results are obtained for $\gamma_0$ and $\gamma_2$). Using Fig. 1, as well as the radial distribution function $[g(r)]$ and diffusion constant $(D)$, we can identify a glassy phase from $T=0$ up to $T_g\approx 1.1$. Above $T_g$ there is a trough in $\langle U\rangle$ up to the melting point $T_m=2.48$, where a discontinuity signals a first-order transition. The insets of Fig. 1 show the separate contributions from $A$-$A$, $A$-$B$, and $B$-$B$ bonds. Clearly, $\langle U_{BB}\rangle$ increases for $T>T_g$, which means that $B$ particles are getting closer. They have a high $D$ as shown by the red circles presented in Fig. 2. Most $A$ particles begin to

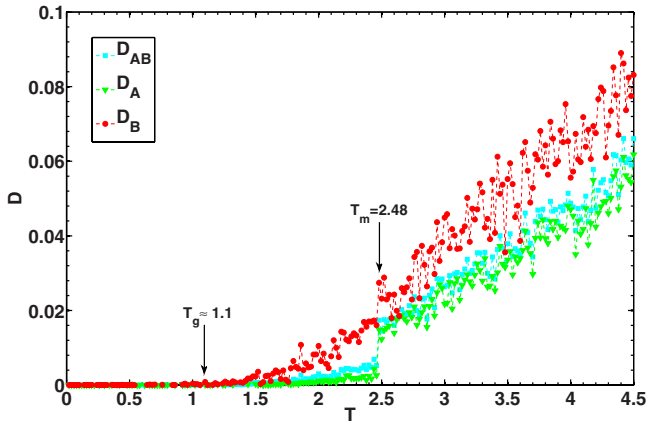


FIG. 2. (Color online) Diffusion constant $D$ as a function of the temperature. Triangles are particles $A$ $(D_A)$, circles are particles $B$ $(D_B)$, and squares are the whole mixture $D_{AB}$.

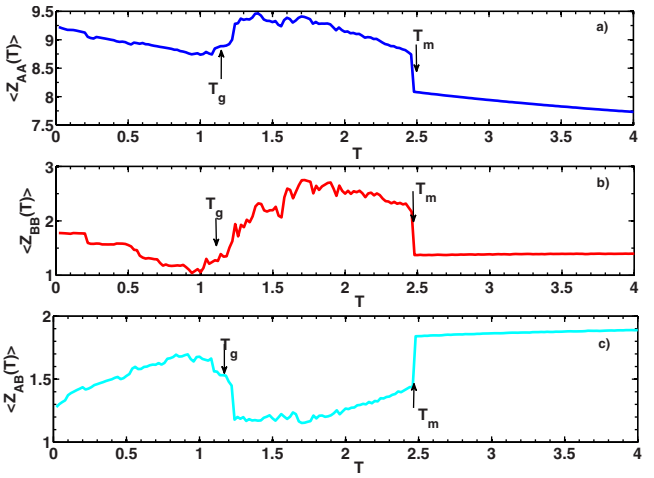


FIG. 3. (Color online) Nearest neighbors $\langle Z\rangle$ of (a) type $A$ around $A$, (b) type $B$ around $B$, and (c) type $B$ around $A$. We can see an increase in $\langle Z_{AA}\rangle$ above $T_g$. A similar behavior is shown in (b), however, $B$ spheres have more mobility, like in a fluid. A decrease is observed in $\langle Z_{AB}\rangle$ indicating phase separation.

crystallize for $T>T_g$, since a second peak in $g(r)$ appears at roughly[24] $r\approx\sqrt{2}$ which is a typical mark of the second-nearest neighbors in a fcc crystal. Thus, the nature of the dynamics for $T_m>T>T_g$ is basically a relaxation toward phase separation, in which $B$ particles leave the cages inside the glass by diffusive processes, while at the same time, the rigid backbone of $A$ sites begins to crystallize with abrupt shocks.[25]

We can connect these processes with the BP and the rigidity of the network. Figure 3 shows the evolution of $\langle Z\rangle$ for each atomic species and kind of bonds, obtained from,

$$\langle Z_{\alpha\beta}\rangle=\int_0^{r^c_{\alpha\beta}}4\pi r^2 g_{\alpha_\beta}(r)dr. \tag{2}$$

It is important to remark that here we integrate using the cut-off given by $\Phi_{\alpha\beta}(r_{ij})$. This is a critical fact, since it allows to define what is a contact in the sense of RT. Notice that here we do not consider angular constraints due to the radial nature of the potential, although there is a certain amount of indirect angular constraints for some configurations due to geometrical hindrance.[18] The main reason to not consider such effect is the temperature dependence of the corresponding constraints, since they are broken at much lower temperatures[18] than $T_g$. In principle, all active constraints at a given temperature can be counted using a thermodynamical integration procedure.[26,27]

In Fig. 3(a), the number of $A$ nearest neighbors of $A$ increases when $T>T_g$ while Fig. 3(b) shows how $\langle Z_{BB}\rangle$ also increases in spite of a higher mobility while $\langle Z_{AB}\rangle$ decreases. This indicates phase separation, since $A$ and $B$ particles tend to form separate crystals, increasing their respective coordination with atoms of the same type.

According to RT, changes in coordination are reflected in the presence of LFVM. To test this, we obtained the vibrational density of states $g(\omega)$, calculated always in metastable states,[24] using the Fourier transform of the velocity autocor-

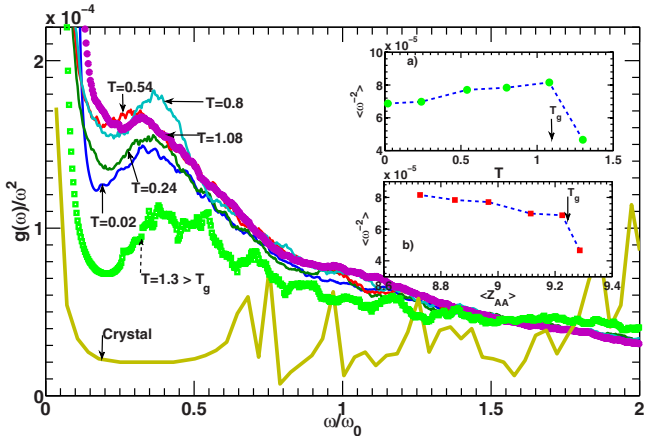


FIG. 4. (Color online) Reduced density of vibrational modes $g(\omega)/\omega^2$ for glasses at different temperatures. At $T=1.3>T_g$, there is a reduction in the Boson peak with respect to temperatures below $T_g$. $\omega_0$ is a characteristic frequency. For comparison, the result obtained for a crystal at low $T$ is presented. Inset (a): evolution of the $\langle\omega^{-2}\rangle$ at low frequencies as a function of the temperature $T$. Inset (b): the same quantity but now in function of the coordination number $\langle Z_{AA}\rangle$.

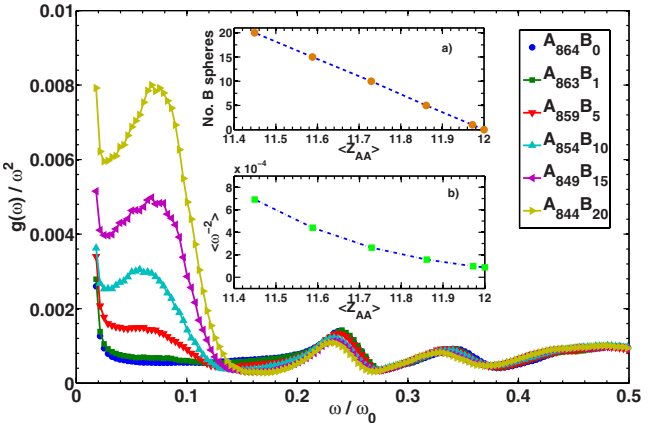


FIG. 5. (Color online) Reduced density of vibrational modes $g(\omega)/\omega^2$ for a fcc lattice of $A$ atoms with a concentration $x$ of $B$ atoms with a reduced diameter. The number of $B$ particles is indicated in the inset for each curve. Inset (a): number of $B$ atoms as a function of the average coordination. Inset (b): evolution of the $\langle\omega^{-2}\rangle$ at low frequencies as a function of the coordination number $\langle Z_{AA}\rangle$.

relation function.[28] Figure 4 shows the reduced density of vibrational modes $g(\omega)/\omega^2$ for different $T$. For the glass, two peaks appear in the low-frequency region, one at $\omega=0$, known as the quasielastic peak,[28] due to the motion outside the range of the potential. The other one is the BP.[28] With color curves indicated by arrows, we show the evolution of the BP with increasing $T$, and in the inset of Fig. 4(a), the evolution of the integral $\int g(\omega)/\omega^2 d\omega \equiv \langle\omega^{-2}\rangle$ (at low frequencies) over the same temperatures. $\langle\omega^{-2}\rangle$ grows from $T=0$ to $T\approx 1$, which correlates well with the decrease in the coordination numbers $\langle Z_{AA}\rangle$ and $\langle Z_{BB}\rangle$, Fig. 4(b). $\langle Z_{AB}\rangle$ also grows but the number of such bonds is much smaller than the number of $A$-$A$ bonds.

The rise of the BP leads to decreased mechanical stability. For $T>T_g$, the height of the BP is dramatically reduce, for example at $T=1.3$, as shown in Fig. 4, while at the same time $\langle Z_{AA}\rangle$ and $\langle Z_{BB}\rangle$ rise. This is caused by phase separation and a tendency for crystallization, as can be seen when we compare with a pure fcc of pure $A$ particles (Fig. 4). On average the mixture has more contacts above $T_g$ and as a consequence, the BP is smaller. The reduction in BP height for $T=1.3>T_g$ is about 40%, when compared to the peak at $T_g$. Another important feature is the change in position of the BP with temperature, in agreement whit experiment.[29] Because of the phase-separation values of BP for $T>1.3$ are not attainable by heating. However, it appears that $\langle\omega^{-2}\rangle$ extrapolates to a small value near the onset of $B$ atom diffusivity near $T=1.5$ (Fig. 2).

The BP can be connected to the coordination number by starting a fcc made from pure $A$ atoms near $T=0$. Choose atoms at random with a given concentration $(x)$ and reduce the size of the chosen atoms to make them $B$ atoms. To avoid energetic effects due to different bonds, set $\epsilon_{AA}=\epsilon_{BB}=\epsilon_{AB}$. Figure 5 shows $g(\omega)/\omega^2$ for small concentrations $x$ of $B$ atoms. The height of the BP and its frequency increase with $x$, in agreement with experiment.[30] Figure 5(b) shows a linear relationship between the value $\langle\omega^{-2}\rangle$ at low frequencies and the coordination number $\langle Z_{AA}\rangle$. When the lattice is softer (lower coordination) low-frequency modes appear, seen as a peak in $g(\omega)/\omega^2$. Thus, the lack of contacts is important in both the crystal or glass. The position and height of the resulting BP can be estimated using perturbation theory for the Greens's function $G_0(\mathbf{k},\omega)$ in a fcc lattice with bond defects.[24] The results show that the BP consists of resonant states, with a width which goes as $\Gamma\approx k^4$ (where $k$ is the wave vector), in agreement with the Rayleigh scattering for the phonon inverse mean free path for BP states.[31]

The connection of $T_g$ with the BP and rigidity can be obtained through $\langle u^2(T)\rangle$. For a solid in a given inherent structure, the system can be described by a harmonic Hamiltonian.[32] In that case,

$$\langle u^2(T)\rangle_R \equiv \frac{\langle u^2(T)\rangle}{a^2} \approx \rho^{2/3}\frac{3k_BT}{\langle m\rangle}\int_0^\infty \frac{g(\omega)}{\omega^2}d\omega, \qquad (3)$$

where the value of $a$ is obtained from the position of the first peak of $g_{AB}(r)$, $m$ the mass, and $\rho$ the density. Due to the $1/\omega^2$ factor in Eq. (3), any enhancement of $g(\omega)$ in the low-frequency region leads to a larger $\langle u^2(T)\rangle$.

Figure 6 shows $\langle u^2(T)\rangle_R$ as a function of $T$, calculated using different techniques. First we calculated $\langle u^2(T)\rangle_R$ directly form the particle positions at short times (1200 computer steps), and on short times at inherent structures, obtained through a maximal gradient technique. The almost linear dependence of $T$ indicates that the system behaves as a harmonic system for short times, as predicted by the $T$ dependence in Eq. (3). Second, from Eq. (3) it seems that the excess of LFVM can produce an increased $\langle u^2(T)\rangle_R$ with respect to a crystal. To test this hypothesis, let us calculate $\langle u^2(T)\rangle_R$ from $g(\omega)/\omega^2$ by using Eq. (3) with $g(\omega)$ calculated from the simulations (see Fig. 6). The result can be seen in Fig. 6 with red diamonds for the mixture and blue triangles for $A$ spheres. There is good agreement between $\langle u^2(T)\rangle_R$

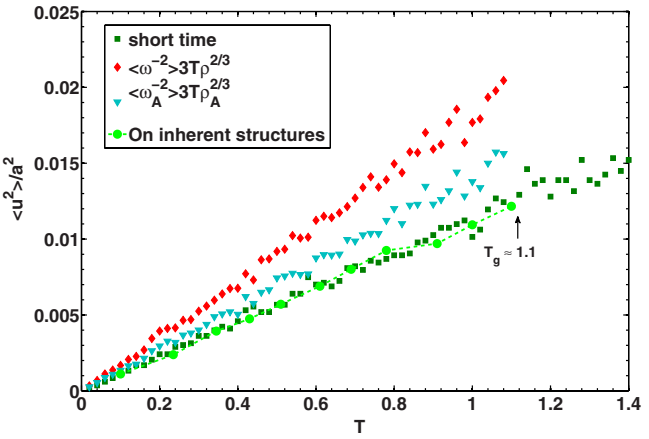


FIG. 6. (Color online) Square mean displacement. Green squares represent short scales of time while green circles show $\langle u^2 \rangle$ on the inherent structures. On the same plot, with red diamonds and downward triangles, we present the same quantity calculated from $g(\omega)$ and $g_A(\omega)$, using Eq. (3).

obtained from the particle trajectories and those obtained from $g(\omega)$, specially if only the rigid backbone of sites $A$ is considered.

Now that we have shown that Eq. (3) is a good approximation for $\langle u^2(T) \rangle_R$ we can understand how the excess of modes is related to $T_g$. From experiments and simulations, it is known that $T_g$ can be estimated from the Lindemann criteria,[20,32,33] which establishes that the glass transition happens at $\sqrt{\langle u^2(T_g) \rangle}/a^2 \approx 0.15$. From this criteria and Eq. (3) $T_g$ is given by $T_g \approx 0.05 \langle m \rangle / \rho^{2/3} k_B \int_0^\infty g(\omega)/\omega^2 d\omega$. Thus, Fig. 6 can be used to estimate $T_g$ from the vibrational properties via $g(\omega)$. We only need to look at the temperature where $\sqrt{\langle u^2(T) \rangle}_R \approx 0.15$. Using Fig. 6, it follows that $T_g \approx 1.0$ if $g(\omega)$ is used. When $g_A(\omega)$ is considered, $T_g$ is given by 1.1. In both cases, the agreement is excellent with the $T_g$ obtained from the thermodynamical behavior. Thus, the BP has an impact in $T_g$ through a softening of the vibrational modes, which leads to an increased displacement of the atoms. The present results are connected to the glass viscosity ($\eta$) and fragility, since there is an almost universal scaling[4] of $\langle u^2(T) \rangle_R$ with $\eta$.

## IV. CONCLUSIONS

In network glasses constraint theory identifies the BP floppy modes and predicts their dependence on $\langle Z \rangle$ in good agreement with neutron-scattering experiment.[34–37] Network glasses with noncentral forces are not easily simulated on computationally accessible time scales, so here we have tasted these ideas on popular bidispersive spherical (central force) glasses. By heating the solids spherical glass trough $T_g$ we have demonstrated a correlation between $\langle Z \rangle$ and the evolution of the BP, showing that the BP is not caused merely by randomness-induced redistribution of vibrational frequencies, as has been suggested recently.[38] Moreover, it appears that these $\langle Z \rangle$ correlations are likely to be a universal property of all good glass formers, contrary to the suggestion that "there is nothing universal about the temperatures dependence of the specific heat in glass formers."[39] The softening of the vibrational modes leads to increased mean quadratic displacements, and $T_g$ can be estimated from such softening. Finally, it is worthwhile mentioning that although our simulations were performed under constant volume conditions, almost all experiments are conducted under constant pressure conditions. Under such realistic conditions, the average connectivity is changed, and thus a shift of the Boson peak and $T_g$ can be expected.

## ACKNOWLEDGMENTS

We thank DGAPA-UNAM under Project No. IN-1003310-3. The calculations were performed at Kanbalam and Bakliz supercomputers at DGSCA-UNAM.

[1] J. Langer, Phys. Today **60**(2), 8 (2007).
[2] P. K. Gupta and J. C. Mauro, J. Chem. Phys. **130**, 094503 (2009).
[3] J. C. Phillips, Rep. Prog. Phys. **59**, 1133 (1996).
[4] L. Larini, A. Ottochian, C. De Michele, and D. Leporini, Nat. Phys. **4**, 42 (2007).
[5] J. R. Romero-Arias and G. G. Naumis, Phys. Rev. E **77**, 061504 (2008).
[6] M. I. Klinger, Phys. Rep. **492**, 111 (2010).
[7] G. D'Angelo, G. Carini, C. Crupi, M. Koza, G. Tripodo, and C. Vasi, Phys. Rev. B **79**, 014206 (2009).
[8] J. C. Phillips, J. Non-Cryst. Solids **34**, 153 (1979).
[9] M. F. Thorpe, J. Non-Cryst. Solids **57**, 355 (1983).
[10] D. Selvanathan, W. J. Bresser, and P. Boolchand, Phys. Rev. B **61**, 15061 (2000).
[11] Y. Wang, J. Wells, D. G. Georgiev, P. Boolchand, K. Jackson, and M. Micoulaut, Phys. Rev. Lett. **87**, 185503 (2001).
[12] D. I. Novita, P. Boolchand, M. Malki, and M. Micoulaut, Phys. Rev. Lett. **98**, 195501 (2007).
[13] M. Wyart, Ann. Phys. **30**, 1 (2005).
[14] N. Xu, M. Wyart, A. J. Liu, and S. R. Nagel, Phys. Rev. Lett. **98**, 175502 (2007).
[15] K. Lu, E. E. Brodsky, and H. P. Kavehpour, Nat. Phys. **4**, 404 (2008).
[16] A. Huerta and G. G. Naumis, Phys. Rev. Lett. **90**, 145701 (2003).
[17] A. Huerta, G. G. Naumis, D. T. Wasan, D. Henderson, and A. Trokhymchuk, J. Chem. Phys. **120**, 1506 (2004).
[18] A. Huerta and G. G. Naumis, Phys. Rev. B **66**, 184204 (2002).
[19] P. G. Debenedetti, *Metastable Liquids* (Princeton University Press, Princeton, 1996).
[20] G. G. Naumis, Phys. Rev. B **73**, 172202 (2006).
[21] G. G. Naumis, J. Non-Cryst. Solids **352**, 4865 (2006).
[22] G. G. Naumis, Phys. Rev. B **61**, R9205 (2000).
[23] K. Vollmayr, W. Kob, and K. Binder, J. Chem. Phys. **105**, 4714 (1996).

[24] H. M. Flores-Ruiz and G. G. Naumis (unpublished).
[25] C. Brito and M. Wyart, J. Stat. Mech.: Theory Exp. 2007, L08003.
[26] G. Foffi and F. Sciortino, Phys. Rev. E **74**, 050401(R) (2006).
[27] G. Foffi, J. Phys.: Condens. Matter **20**, 494241 (2008).
[28] S. V. Meshkov, Phys. Rev. B **55**, 12113 (1997).
[29] A. I. Chumakov, I. Sergueev, U. van Bürck, W. Schirmacher, T. Asthalter, R. Rüffer, O. Leupold, and W. Petry, Phys. Rev. Lett. **92**, 245508 (2004).
[30] P. Chen, C. Holbrook, P. Boolchand, D. G. Georgiev, K. A. Jackson, and M. Micoulaut, Phys. Rev. B **78**, 224208 (2008).
[31] K. Binder and W. Kob, *Glassy Materials and Disordered Solids* (World Scientific, Singapore, 2005).
[32] G. G. Naumis and H. M. Flores-Ruiz, Phys. Rev. B **78**, 094203 (2008).
[33] U. Buchenau and R. Zorn, Europhys. Lett. **18**, 523 (1992).
[34] W. A. Kamitakahara, R. L. Cappelletti, P. Boolchand, B. Halfpap, F. Gompf, D. A. Neumann, and H. Mutka, Phys. Rev. B **44**, 94 (1991).
[35] L. Orsingher, G. Baldi, A. Fontana, L. E. Bove, T. Unruh, A. Orecchini, C. Petrillo, N. Violini, and F. Sacchetti, Phys. Rev. B **82**, 115201 (2010).
[36] E. L. Gjersing, S. Sen, and R. E. Youngman, Phys. Rev. B **82**, 014203 (2010).
[37] P. Boolchand, G. Lucovsky, J. C. Phillips, and M. F. Thorpe, Philos. Mag. **85**, 3823 (2005).
[38] V. Ilyin, I. Procaccia, I. Regev, and Y. Shokef, Phys. Rev. B **80**, 174201 (2009).
[39] H. G. E. Hentschel, V. Ilyin, and I. Procaccia, Phys. Rev. Lett. **101**, 265701 (2008).